Nanocrystals of diluted magnetic semiconductors: Model for magnetic polaron

A. K. Bhattacharjee
Laboratoire de Physique des Solides, Université Paris-Sud, 91405 Orsay, France
(Received 14 September 1994)

We present a simple model for the magnetic polaron associated with an electron-hole pair in a semimagnetic semiconductor quantum dot. An exactly soluble Hamiltonian based on the effective-mass approximation is used to calculate the equilibrium properties. The polaron binding energy decreases with increasing temperature or magnetic field. Low-temperature magnetization and luminescence polarization show rapid saturation with magnetic field. Strong light-induced enhancement of magnetization is predicted.

Semiconductor nanocrystallites, also called quantum dots (QD's), have been the subject of intense activity in recent years.[1] In the strong confinement regime, when the QD radius is much smaller than the bulk exciton Bohr radius, the excitonic effect is negligible and linear optical absorption corresponds to electric-dipole transitions from discrete valence-band levels to discrete conduction-band levels.[2] The fundamental gap for the creation of an electron-hole pair in a QD is higher than that in the bulk. This confinement-induced blueshift increases with decreasing QD size. High-quality nanocrystallites of II-VI compounds have been fabricated and their optical properties investigated in great detail.[3] In particular, well-characterized band-edge luminescence has been observed in CdSe QD's. On the other hand, semimagnetic or diluted magnetic semiconductors (DMS's) based on II-VI compounds, such as $Cd_{1-x}Mn_xTe$, are known for giant magneto-optical properties and magnetic polarons.[4] These effects arise from strong *sp-d* exchange interactions between the band carriers and the Mn^{2+} ions. Bound magnetic polarons associated with shallow impurities (donors and acceptors) have been extensively studied. Localized exciton magnetic polarons have also been reported in bulk and epilayer $Cd_{1-x}Mn_xTe$ (Ref. 5) and in $CdTe/Cd_{1-x}Mn_xTe$ heterostructures.[6] Acceptor-bound magnetic polarons approach the saturation regime at low temperature;[7–13] the mutual spin polarization between the bound hole and the Mn ions situated in its orbit tends to form a ferromagnetic cluster. A similar situation is expected in an optically excited small DMS nanocrystal, with an additional contribution from the electron. In fact, such a QD should be a model for zero-dimensional exciton magnetic polaron, provided the polaron formation time is shorter than the lifetime of the electron-hole pair.

Wang *et al.*[14] reported the first experimental investigation of DMS nanocrystals. $Zn_{0.93}Mn_{0.07}S$ crystallites of average diameter $\simeq 25$ Å were grown in a glass matrix. The observed photoluminescence (PL) peak at 2.12 eV corresponds to the well-known Mn^{2+} internal emission. The PL excitation spectrum yielded a quantum-confinement blueshift of 0.23 eV for the fundamental gap. They also measured the static magnetic susceptibility from 2.3 K to 314 K; the data fit the Curie-Weiss law with a negligibly small Θ value, suggesting a smaller contribution of the antiferromagnetic Mn-Mn interaction in the QD than in the bulk. More recently, Bhargava *et al.*[15] fabricated coated Mn-doped ZnS particles of diameter varying from 35 to 75 Å. They focused on the characteristics of the Mn^{2+} luminescence: a high luminescence efficiency and a dramatically short decay time were observed. They also noted a negligible shift of the PL-excitation (PLE) spectrum in a magnetic field. The latter effect might be related to the formation of magnetic polaron, as we shall see. However, $Zn_{1-x}Mn_xS$ with the bulk band gap above 3.8 eV seems unsuitable for studying the magnetic polaron, because the PL spectrum is dominated by the Mn emission. Moreover, the time of energy transfer from an electron-hole pair to the Mn *d* shell is short (< 500 psec),[15] perhaps in the range of the polaron formation time (~ 100 psec in the bulk).[5] $Cd_{1-x}Mn_xTe$ should be a better candidate for realizing the magnetic polaron in a QD. CdTe nanocrystallites have been already investigated;[3,16] the strong confinement regime is easily attained, the bulk exciton Bohr radius being ~ 70 Å. It should be possible to choose the composition (x) and size in order to have QD's with a fundamental gap below the Mn^{2+} excitation. The theoretical estimate[17] of the time for the radiative recombination of an electron-hole pair is in the nanosecond range. Thus magnetic polaron formation is expected and its properties might be investigated through the band-edge luminescence of the QD.

To our knowledge, no theoretical study of semimagnetic QD's has yet been reported. Here we present a simple model for magnetic polaron associated with an electron-hole pair. The thermodynamical equilibrium properties of the polaron are calculated. We also calculate the Zeeman splitting of the exciton in the QD. We first summarize the theoretical model and then present some numerical results for $Cd_{1-x}Mn_xTe$ quantum dots.

Theoretical studies of the electronic structure of nonmagnetic semiconductor QD's have been based on either the effective-mass approximation[2] (EMA) or the tight-binding method.[18] The EMA is known to grossly overestimate the confinement energies in small QD's. However, the EMA wave functions have been found to be sufficiently accurate for the optical properties.[19] Our model for semimagnetic QD's is based on the EMA wave functions for a spherical dot[17] of radius a. The lowest

 ©1995 The American Physical Society

conduction-band level corresponds to

$$\Psi_m^c(\mathbf{r}) = f(\mathbf{r})u_m^c(\mathbf{r}), \tag{1}$$

where the envelope function

$$f(\mathbf{r}) = \sqrt{\frac{2}{a}}\frac{\sin(\pi r/a)}{r}Y_{00} \tag{2}$$

and $u_m^c(\mathbf{r})$ is the periodic part of the Bloch function at Γ, with $m = \pm\frac{1}{2}$. In the spherical approximation the wave functions for the highest odd-parity valence-band level are

$$\Psi_\mu^v(\mathbf{r}) = \sum_\nu F_{\nu\mu}(\mathbf{r})u_\nu^v(\mathbf{r}), \tag{3}$$

where μ,ν run through $\frac{3}{2}$, $\frac{1}{2}$, $-\frac{1}{2}$, and $-\frac{3}{2}$,

$$F_{\nu\mu}(\mathbf{r}) = 2(-1)^{\mu-\frac{3}{2}}\left[R_0(r)\begin{pmatrix}\frac{3}{2} & 0 & \frac{3}{2}\\ \nu & 0 & -\mu\end{pmatrix}Y_{00} + R_2(r)\begin{pmatrix}\frac{3}{2} & 2 & \frac{3}{2}\\ \nu & \mu-\nu & -\mu\end{pmatrix}Y_{2,\mu-\nu}(\theta,\phi)\right], \tag{4}$$

where Wigner's $3j$ symbols have been used. The exchange interaction between a band electron (spin $s = \frac{1}{2}$) and the Mn d electrons (total ionic spin $S = \frac{5}{2}$) is given by

$$H_{\text{ex}}^{c,v} = -\sum_i J^{c,v}(\mathbf{r} - \mathbf{R}_i)\mathbf{s}\cdot\mathbf{S}_i, \tag{5}$$

where i labels the Mn ions. We follow the perturbation approach and study its effects on the electron and hole ground-state multiplets, by neglecting mixing with other states. Now,

$$\langle\Psi_m^c|H_{\text{ex}}^c|\Psi_n^c\rangle = -\alpha\sum_i |f(\mathbf{R}_i)|^2\langle m|\mathbf{s}\cdot\mathbf{S}_i|n\rangle, \tag{6}$$

where $|m\rangle$ is an eigenstate of s_z and $\alpha = \langle u_s|J^c(\mathbf{r})|u_s\rangle$, with $|u_s\rangle$ for the s-like orbital wave function. Similarly,

$$\langle\Psi_\mu^v|H_{\text{ex}}^v|\Psi_\nu^v\rangle = -\frac{\beta}{3}\sum_{i,\lambda,\xi} F_{\lambda,\mu}^*(\mathbf{R}_i)\langle\lambda|\mathbf{j}\cdot\mathbf{S}_i|\xi\rangle F_{\xi,\nu}(\mathbf{R}_i), \tag{7}$$

where $|\mu\rangle$ is an eigenstate of j_z ($j = \frac{3}{2}$) and $\beta = \langle u_x|J^v(\mathbf{r})|u_x\rangle$. The Mn spin system is described in terms of the individual $S_{iz} = m_i$ values:

$$\Psi_{\text{Mn}} = \prod_{i=1}^N |m_i\rangle, \tag{8}$$

where N is the total number of Mn ions in the QD. At low Mn concentration (x), the antiferromagnetic interaction between the Mn spins can be neglected, more so in a QD than in the bulk.[14] For a magnetic field B in the z direction the Zeeman Hamiltonian

$$H_Z = \mu_B g_{\text{Mn}} B\sum_{i=1}^N S_{iz}. \tag{9}$$

The direct effect of the magnetic field on the electron states is small. In the mean-field approximation $\mathbf{S}_i$ in Eqs. (6) and (7) is replaced by the average (thermodynamic and configurational) value $\hat{\mathbf{z}}\langle S_z\rangle$. Replacing the sum over i by an integral, we obtain the Zeeman splittings

$$E_m^c = -(N_0 x\alpha)m\langle S_z\rangle \tag{10}$$

and

$$E_\mu^v = -\rho(N_0 x\beta/3)\mu\ \langle S_z\rangle. \tag{11}$$

Here N_0 is the number of primitive cells per unit volume in the DMS crystal. The reduction factor ρ for the valence-band states is given by

$$\rho = \frac{1}{\mu}\sum_\nu \nu\int |F_{\nu,\mu}(\mathbf{r})|^2 d\mathbf{r}. \tag{12}$$

Straightforward calculation yields

$$\rho = \int_0^a \left(|R_0(r)|^2 + \frac{1}{5}|R_2(r)|^2\right) r^2 dr. \tag{13}$$

This is simply related to the function $v(\gamma)$ calculated by Efros:[17]

$$\rho = \frac{1}{2}[1 + v(\gamma)], \tag{14}$$

where γ is the ratio of the light- and heavy-hole effective masses. For CdTe, $\gamma \simeq 0.16$ and $\rho \simeq 0.8$. We have thus shown that the Zeeman splitting of the valence-band edge in a QD is smaller than that in the bulk DMS. A similar reduction factor was previously obtained[20] for an acceptor-bound hole.

In order to study the magnetic polaron it is necessary to go beyond this mean-field approximation. The Hamiltonian representing the polaron associated with an electron-hole pair is given by the difference $(H_{\text{ex}}^c - H_{\text{ex}}^v)$, with $\mathbf{j}$ of the valence-band electron going to $-\mathbf{j}$ for the hole. An exactly soluble model is obtained by resorting to a constant-coupling approximation that becomes exact in the saturation limit. It can be written as

$$H_{\text{pol}} = -I_c(\mathbf{s}\cdot\mathbf{\Sigma}) + I_v(\mathbf{j}\cdot\mathbf{\Sigma}), \tag{15}$$

where

$$\mathbf{\Sigma} = \sum_i \mathbf{S}_i \tag{16a}$$

with $\Sigma = NS, NS-1, NS-2, ..., 0$ (1/2) for even (odd) N,

$$I_c \equiv \frac{\alpha}{V} = \frac{N_0\alpha x}{N}, \tag{16b}$$

where V is the QD volume, and

$$I_v \equiv -\rho\frac{\beta}{3V} = -\rho\frac{N_0\beta x}{3N}. \tag{16c}$$

Note that the isotropic spin Hamiltonian $H_{\rm pol}$ applies to zinc-blende DMS's such as $Cd_{1-x}Mn_xTe$; for wurtzite DMS's such as $Cd_{1-x}Mn_xSe$ it is necessary to add a crystal-field term Dj_z^2 that represents the splitting between the A and B valence bands.[13] It has been shown, however,[17] that the splitting is reduced in a QD by the factor $v(\gamma)$, which is $\simeq 0.4$ for CdSe.

The Zeeman Hamiltonian can be rewritten as

$$H_Z = \mu_B g_{Mn} B\Sigma_z \ . \tag{17}$$

In the absence of the magnetic field, $H_{\rm pol}$ represents the total polaron Hamiltonian in a zinc-blende DMS nanocrystal. Noting that $\mathbf{J} \equiv \mathbf{s} + \mathbf{j} + \mathbf{\Sigma}$ commutes with $H_{\rm pol}$, the polaron eigenvalues and eigenstates can be deduced analytically by using the theory of addition of three angular momenta. In fact, the good quantum numbers are s, j, Σ, J, and $M = J_z$. We first add $\mathbf{s}$ and $\mathbf{\Sigma}$ to obtain σ_s. In nontrivial cases the two values $\sigma_s = \Sigma \pm \frac{1}{2}$ are compatible with a given J. This leads to a 2×2 matrix for a given set of (J, M). The matrix elements of $\mathbf{j} \cdot \mathbf{\Sigma}$ are calculated by using the Racah coefficients.[21] The two energy levels for a given (J, M) are

$$\begin{aligned}\Lambda_\pm(\Sigma, J) = {} & \frac{I_c}{4} + \frac{I_v}{2}[(J+\tfrac{1}{2})^2 - (\Sigma+\tfrac{1}{2})^2 - \tfrac{7}{2}] \\ & \pm\tfrac{1}{2}\{[(\Sigma+\tfrac{1}{2})I_c + (J+\tfrac{1}{2})I_v]^2 \\ & + I_c I_v[(J-\Sigma)^2 - 4]\}^{\frac{1}{2}}.\end{aligned} \tag{18}$$

The corresponding eigenstates are linear combinations of $|\sigma_s = \Sigma + \frac{1}{2}, j = \frac{3}{2}, J, M\rangle$ and $|\sigma_s = \Sigma - \frac{1}{2}, j = \frac{3}{2}, J, M\rangle$. The ground state of the polaron is given by $\Sigma = NS$ and $J = \Sigma - 1$ with the energy

$$E_0 = \Lambda_-(NS, NS-1) \tag{19}$$

with all Mn spins aligned parallel to the electron spin and antiparallel to the hole angular momentum. We shall see that the magnetic behavior at low temperature is superparamagnetic with the cluster spin NS. The first excited state of the polaron is given by $\Sigma = NS - 1$ and $J = \Sigma - 1$. The excitation energy decreases with increasing QD size. The highest-energy states correspond to $\Sigma = NS$ and $J = \Sigma + 1$ with the energy $E_{\rm max} = \Lambda_+(NS, NS+1) \simeq -E_0$. Note that in order to calculate the partition function we also need the number of ways $b(\Sigma)$ to obtain a given value of Σ out of N spins S. It is given by

$$b(\Sigma) = a(\Sigma) - a(\Sigma+1), \tag{20}$$

where $a(\sigma)$ is the coefficient of X^σ in the expansion of $(X^{-S} + X^{-S+1} + \cdots + X^S)^N$.

In the presence of a magnetic field and/or uniaxial distortion (Dj_z^2), J is no longer a good quantum number, but $M = J_z$ is. The polaron eigenvalue problem can then be solved by numerical diagonalization of 8×8 or smaller matrices. The calculations are similar to those for an acceptor-bound polaron.[13]

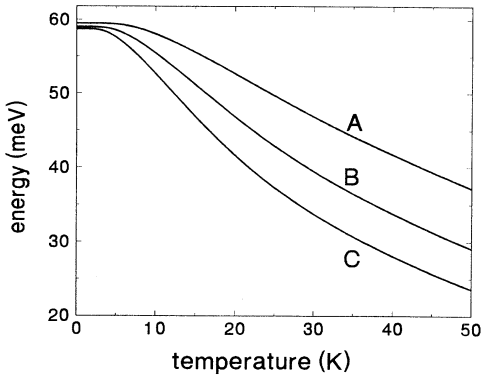

FIG. 1. Polaron binding energy (meV) vs temperature (K) in $Cd_{0.95}Mn_{0.05}Te$ quantum dots. Curves A, B, and C correspond to the dot radius $a = 15$, 16.5, and 18 Å, respectively.

Here we present some results for nanocrystals of $Cd_{0.95}Mn_{0.05}Te$ with $N_0\alpha = 0.22$ eV and $N_0\beta = -0.88$ eV. The thermodynamic equilibrium properties of the magnetic polaron are calculated. Figure 1 shows the zero-field binding energy as a function of temperature for different QD sizes: $a = 15$, 16.5, and 18 Å with $N = 10$, 14, and 18, respectively. The binding energy decreases faster in larger QD's, because the energy levels get closer. Experimentally, the polaron binding energy should be observable as a redshift of the PL peak with respect to the absorption or PLE maximum. Time-resolved PL seems to be the most appropriate tool for investigating the polaron dynamics.[5] Figure 2 presents the polaron binding energy as a function of magnetic field at different temperatures: $T = 1.8$, 4.2, and 10 K for a QD with $N = 10$. It is obtained by subtracting the Zeeman shift $\frac{1}{2}(I_c + 3I_v)|\langle\Sigma_z\rangle|$ of the electron-hole excitation energy from $|\langle H_{\rm pol}\rangle|$. Notice how rapidly the polaron shift vanishes with applied field at low temperature. It is tempting to relate this effect to the reported absence of magneto-

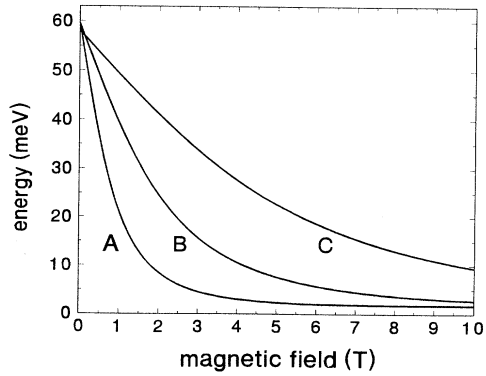

FIG. 2. Polaron binding energy (meV) vs magnetic field (tesla) in $Cd_{0.95}Mn_{0.05}Te$ quantum dots of radius 15 Å. Curves A, B, and C correspond to $T = 1.8$, 4.2, and 10 K, respectively.

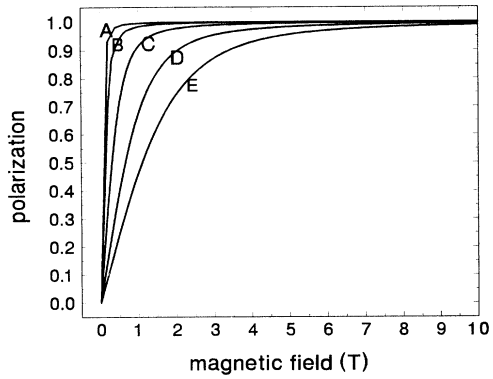

FIG. 3. Degree of circular polarization of the electron-hole pair luminescence in $Cd_{0.95}Mn_{0.05}Te$ quantum dots of radius 15 Å vs magnetic field. Curves A, B, C, D, and E correspond to $T = 1.8$, 4.2, 10, 20, and 30 K, respectively.

luminescence in ZnS:Mn quantum dots.[15]

Figure 3 shows the field dependence of the degree of circular polarization of the recombination radiation in a QD with $N = 10$ at different temperatures. It is calculated from the relation

$$P_c = \frac{3[n(\frac{3}{2},-\frac{1}{2}) - n(-\frac{3}{2},\frac{1}{2})] + [n(\frac{1}{2},\frac{1}{2}) - n(-\frac{1}{2},-\frac{1}{2})]}{3[n(\frac{3}{2},-\frac{1}{2}) + n(-\frac{3}{2},\frac{1}{2})] + [n(\frac{1}{2},\frac{1}{2}) + n(-\frac{1}{2},-\frac{1}{2})]}, \tag{21}$$

where $n(\mu, m)$ is the equilibrium probability of finding the hole in the state $j_z = \mu$ and the electron in the state $s_z = m$. Equation (21) follows from the well-known relative intensities of the σ^+ and σ^- components of electric dipole transition, which have been shown to remain valid in a QD,[17] even though the absolute values are substantially reduced leading to a longer radiative recombination time. The rapid saturation of the low-temperature curves is a characteristic of the magnetic polaron.[13] Figure 4 presents the magnetization curve of a QD containing

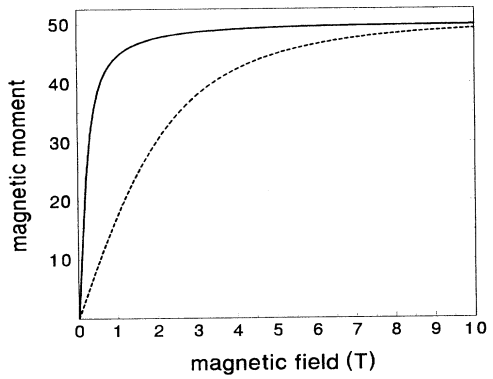

FIG. 4. Average magnetic moment (in Bohr magnetons) of a $Cd_{0.95}Mn_{0.05}Te$ quantum dot of radius 15 Å vs magnetic field at $T = 4.2$ K. The solid curve corresponds to the equilibrium magnetic polaron. The dashed curve corresponds to ordinary paramagnetism. The difference represents the light-induced enhancement of magnetization.

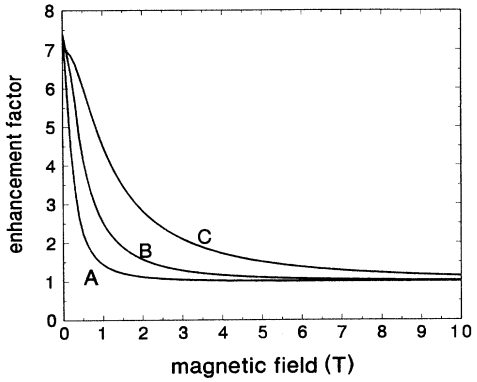

FIG. 5. Light-induced magnetization enhancement factor for a sample containing $Cd_{0.95}Mn_{0.05}Te$ quantum dots of radius 15 Å vs magnetic field. Curves A, B, and C correspond to $T = 1.8$, 4.2, and 10 K, respectively.

$N = 10$ Mn ions at $T = 4.2$ K. The solid curve shows M_P corresponding to the magnetic polaron in equilibrium. The dashed curve shows M obtained from the Brillouin function for spin $S = \frac{5}{2}$ and represents the magnetization in the absence of an electron-hole pair. It is interesting to note that the solid curve is very close to the Brillouin function for the giant spin $\Sigma = NS$, corresponding to the polaron ground state. The low-temperature magnetization is thus superparamagnetic. The difference between the solid and the dashed curves in Fig. 4 represents the light-induced enhancement of magnetization, which might be measured following the method of Wojtowicz *et al.*[22] Figure 5 shows the light-induced magnetization enhancement factor (M_P/M) as a function of magnetic field at different temperatures. Although the ratio of the polaron magnetic moment to the paramagnetic one increases with increasing temperature, in terms of absolute values the light-induced magnetization enhancement should be most important at low T and low B.

In summary, we have developed a simple model for the magnetic polaron associated with an electron-hole pair in a semimagnetic semiconductor nanocrystal. The Zeeman splitting of the exciton is also calculated; it is shown to be reduced with respect to the bulk DMS. We have calculated the equilibrium properties of the magnetic polaron by assuming that the polaron formation time is much shorter than the radiative recombination time. $Cd_{1-x}Mn_xTe$ appears to be a good candidate for experimental realization. The polaronic redshift of the band-edge luminescence is predicted to decrease with increasing temperature or magnetic field. The luminescence polarization, as well as the magnetization, shows rapid saturation at low temperatures. The low-temperature magnetization curves correspond to the superparamagnetism of ferromagnetic cluster associated with the magnetic polaron. A strong light-induced enhancement of magnetization is thus predicted.

The Laboratoire de Physique des Solides is "Unité de Recherche Associée au Centre National de la Recherche Scientifique No. 002."

[1] For a recent review see Y. Wang and N. Herron, J. Phys. Chem. **95**, 525 (1991).
[2] Al. L. Efros and A. L. Efros, Fiz. Tekh. Poluprovodn. **16**, 1209 (1982) [Sov. Phys. Semicond. **16**, 772 (1982)].
[3] C. B. Murray, D. J. Norris, and M. G. Bawendi, J. Am. Chem. Soc. **115**, 8706 (1993); D. J. Norris, A. Sacra, C. B. Murray, and M. G. Bawendi, Phys. Rev. Lett. **72**, 2612 (1994).
[4] For developments until 1986 see *Diluted Magnetic Semiconductors*, edited by J. K. Furdyna and J. Kossut, Semiconductors and Semimetals Vol. 25 (Academic, New York, 1988).
[5] A. Golnik, J. Ginter, and J. A. Gaj, J. Phys. C **16**, 6073 (1983); H. Akinaga, K. Takita, S. Sasaki, S. Takeyama, N. Miura, T. Nakayama, F. Minami, and K. Inoue, Phys. Rev. B **46**, 13 136 (1992); G. Mackh, W. Ossau, D. R. Yakovlev, A. Waag, G. Landwehr, R. Hellmann, and E. O. Göbel, *ibid.* **49**, 10 248 (1994).
[6] D. R. Yakovlev, W. Ossau, G. Landwehr, R. N. Bicknell-Tassius, A. Waag, S. Schmeusser, and I. N. Uraltsev, Solid State Commun. **82**, 29 (1992).
[7] Tran Hong Nhung and R. Planel, Physica B+C **117&118B**, 488 (1983).
[8] A. K. Bhattacharjee, R. Planel, and C. Benoit à la Guillaume, in *Proceedings of the 17th International Conference on the Physics of Semiconductors, San Francisco, 1984*, edited by J. D. Chadi and W. A. Harrison (Springer-Verlag, New York, 1985), p. 1431.
[9] Tran Hong Nhung, R. Planel, C. Benoit à la Guillaume, and A. K. Bhattacharjee, Phys. Rev. B **31**, 2388 (1985).
[10] J. Warnock and P. A. Wolff, Phys. Rev. B **31**, 6579 (1985).
[11] D. Heiman, J. Warnock, P. A. Wolff, R. Kershaw, D. Ridgley, K. Dwight, and A. Wold, Solid State Commun. **52**, 909 (1984).
[12] D. Scalbert, M. Nawrocki, C. Benoit à la Guillaume, and J. Cernogora, Phys. Rev. B **33**, 4418 (1986).
[13] A. K. Bhattacharjee, Phys. Rev. B **35**, 9108 (1987).
[14] Y. Wang, N. Herron, K. Moller, and T. Bein, Solid State Commun. **77**, 33 (1991).
[15] R. N. Bhargava, D. Gallagher, X. Hong, and A. Nurmikko, Phys. Rev. Lett. **72**, 416 (1994).
[16] V. Esch, B. Fluegel, G. Khitrova, H. M. Gibbs, Xu Jiajin, K. Kang, S. W. Koch, L. C. Liu, S. H. Risbud, and N. Peyghambarian, Phys. Rev. B **42**, 7450 (1990).
[17] Al. L. Efros, Phys. Rev. B **46**, 7448 (1992).
[18] P. E. Lippens and M. Lannoo, Phys. Rev. B **39**, 10 935 (1989); **41**, 6079 (1990).
[19] S. V. Nair, L. M. Ramaniah, and K. C. Rustagi, Phys. Rev. B **45**, 5969 (1992).
[20] J. Mycielski and C. Rigaux, J. Phys. (Paris) **44**, 1041 (1983).
[21] M. E. Rose, *Elementary Theory of Angular Momentum* (Wiley, New York, 1961), p. 227.
[22] T. Wojtowicz, S. Kolesnik, I. Miotkowski, and J. K. Furdyna, Phys. Rev. Lett. **70**, 2317 (1993).